Numerical evaluation of truncated Kramers–Kronig transforms

Frederick W. King

Department of Chemistry, University of Wisconsin–Eau Claire, Eau Claire, Wisconsin 54702, USA
fking@uwec.edu

Received December 11, 2006; revised March 5, 2007; accepted March 22, 2007;
posted March 26, 2007 (Doc. ID 77952); published June 15, 2007

The truncated Kramers–Kronig transform, used widely in the analysis of optical data, is recast into a form that avoids the need to evaluate a Cauchy principal-value integral. A specialized Gaussian quadrature involving the weight function $\log_e x^{-1}$ is employed. This approach yields accurate results for functions that lead to kernels with relatively rapid decay, which covers the cases most commonly encountered in optical data analysis. An application to the reststrahlen region of the GaAs spectrum is made. © 2007 Optical Society of America

OCIS codes: 000.4430, 160.4760.

1. INTRODUCTION

One of the standard forms of the Kramers–Kronig transform is given by

$$\mathcal{K}\{\mathcal{O}\}(\omega) = \frac{2}{\pi} P \int_0^\infty \frac{\omega' \mathcal{O}(\omega') \mathrm{d}\omega'}{\omega^2 - \omega'^2}, \tag{1}$$

where P signifies that the Cauchy principal value is taken; $\mathcal{O}(\omega)$ denotes an optical property or, in a more general setting, the dissipative component of a complex property for a causal system; and $\mathcal{K}$ can be regarded as the Kramers–Kronig operator. A slightly modified version of Eq. (1) also arises with the factor ω' replaced by $-\omega$. For general background on the Kramers–Kronig relations, see Peiponen *et al.* [1].

A truncated version of the Kramers–Kronig transform can be written in the form

$$k_{\omega_1,\omega_2}(\omega) \equiv \mathcal{K}_T\{h\}(\omega) = \frac{1}{\pi} P \int_{\omega_1}^{\omega_2} \frac{h(\omega') \mathrm{d}\omega'}{\omega^2 - \omega'^2}, \tag{2}$$

where the circular frequency ω satisfies $0 \le \omega_1 < \omega < \omega_2$ and $k_{\omega_1,\omega_2}(\omega)$ and $h(\omega)$ denote optical properties, though they may also represent other functions for which a Kramers–Kronig analysis is required. The additional factors of 2ω or $2\omega'$ that occur in the standard form of the Kramers–Konig transforms will be incorporated into the functions $k_{\omega_1,\omega_2}(\omega)$ or $h(\omega')$, respectively. To simplify the notation, we replace $k_{\omega_1,\omega_2}(\omega)$ with $k(\omega)$ and adopt this type of notational simplification throughout. Under ideal circumstances, the circular frequency ω_1 should be chosen sufficiently small and the circular frequency ω_2 selected sufficiently large, so that $k_{\omega_1,\omega_2}(\omega)$ is in fact independent of these two frequencies, to a precision level justified by the experimental data. This selection is not always possible because of limitations of the available experimental data or because of difficulties associated with data extrapolation outside the measured spectral range.

In practical applications, two approaches are generally employed for the evaluation of the Kramers–Kronig transform. Experimental data of necessity cannot be measured over a complete spectral domain. One approach handles the missing data region by data extrapolation, which can be aided by the introduction of various physical models of the optical property under investigation. There are several issues associated with this type of extrapolation procedure, and these have been discussed in a number of sources [2,3]. A second approach is to deal with the experimental data at hand, without attempting any extrapolation. This strategy is expected to be successful only when the asymptotic behavior of the optical property falls off quickly outside the measured spectral range. Cases where this is a likely scenario include various nonlinear optical properties [3–5]. To treat the experimental data in the measured spectral range, one can employ two common curve-fitting approaches. In one case, fairly simple functional forms are selected, which allow the truncated Kramers–Kronig transform to be evaluated in closed form. The second situation involves more complicated functional forms in the fitting process, choices that do not allow an analytic solution for the truncated Kramers–Kronig transform to be obtained. In such cases, it is necessary to resort to numerical approaches to evaluate the truncated Kramers–Kronig transform. This particular situation is the subject of the present study. In this work, an efficient and accurate approach is provided to deal with the truncated Kramers–Kronig transform, by reducing it to a specialized Gaussian quadrature.

2. APPROACH

We start by employing a partial fraction resolution of the denominator in Eq. (1), so that

$$k(\omega) = \frac{1}{2\omega\pi} P \int_{\omega_1}^{\omega_2} \frac{h(\omega') \mathrm{d}\omega'}{\omega - \omega'} + \frac{1}{2\omega\pi} \int_{\omega_1}^{\omega_2} \frac{h(\omega') \mathrm{d}\omega'}{\omega + \omega'}. \tag{3}$$

The second integral, which we denote by $k_2(\omega)$, is not a Cauchy principal-value integral and can be dealt with in

a straightforward manner. To treat this integral, employ the change of integration variable

$$\omega' = \tfrac{1}{2}(\omega_1 + \omega_2) + \tfrac{1}{2}(\omega_2 - \omega_1)x; \tag{4}$$

then

$$k_2(\omega) = \frac{(\omega_2 - \omega_1)}{2\omega\pi}\int_{-1}^{1} \frac{h\left(\tfrac{1}{2}[\omega_1 + \omega_2] + \tfrac{1}{2}[\omega_2 - \omega_1]x\right)\mathrm{d}x}{2\omega + \omega_1 + \omega_2 + (\omega_2 - \omega_1)x}. \tag{5}$$

Adopting the same notational simplification employed for $k_{\omega_1,\omega_2}(\omega)$, we introduce the function $\mathcal{O}(\omega,x)$ by the definition

$$\mathcal{O}(\omega,x) = \frac{(\omega_2 - \omega_1)h\left(\tfrac{1}{2}[\omega_1 + \omega_2] + \tfrac{1}{2}[\omega_2 - \omega_1]x\right)}{2\omega\pi\{2\omega + \omega_1 + \omega_2 + (\omega_2 - \omega_1)x\}}; \tag{6}$$

then

$$k_2(\omega) = \int_{-1}^{1} \mathcal{O}(\omega,x)\mathrm{d}x. \tag{7}$$

For all the common optical properties, the function $\mathcal{O}(\omega,x)$ will be a continuous function on the interval $[-1,1]$. In this case the integral can be conveniently evaluated by a Gauss–Legendre quadrature of the form

$$k_2(\omega) \approx \sum_{i=1}^{N} \mathcal{O}(\omega,x_i)w_i, \tag{8}$$

where the weights w_i and evaluation points x_i for a Gauss–Legendre quadrature are readily available for fairly large values of N (see, for example, Stroud and Secrest [6]).

The focus of the remainder of this section is the singular integral appearing in Eq. (3), which we will denote by $k_1(\omega)$. The evaluation strategy to be employed utilizes a specialized Gaussian quadrature, with the integration range restricted to the interval (0,1). However, it will first be useful to put this integral into a standard form that will be amendable to different numerical approaches. Employing the same change of variable indicated in Eq. (4) leads to

$$\begin{aligned} k_1(\omega) &= \frac{1}{2\omega\pi}P\int_{\omega_1}^{\omega_2} \frac{h(\omega')\mathrm{d}\omega'}{\omega - \omega'} \\ &= \frac{1}{2\omega\pi}P\int_{-1}^{1} \frac{h\left(\tfrac{1}{2}[\omega_1 + \omega_2] + \tfrac{1}{2}[\omega_2 - \omega_1]x\right)\mathrm{d}x}{(2\omega - \omega_1 - \omega_2)(\omega_2 - \omega_1)^{-1} - x}. \end{aligned} \tag{9}$$

Using the substitutions

$$x_0 = (2\omega - \omega_1 - \omega_2)(\omega_2 - \omega_1)^{-1}, \tag{10}$$

$$f(x) = h\left(\tfrac{1}{2}[\omega_1 + \omega_2] + \tfrac{1}{2}[\omega_2 - \omega_1]x\right), \tag{11}$$

$$K(x_0) = \{\omega_1 + \omega_2 + x_0(\omega_2 - \omega_1)\}k_1\left(\tfrac{1}{2}[\omega_1 + \omega_2] + \tfrac{1}{2}[\omega_2 - \omega_1]x\right), \tag{12}$$

then

$$K(x_0) = \frac{1}{\pi}P\int_{-1}^{1} \frac{f(x)\mathrm{d}x}{x_0 - x}, \tag{13}$$

where $-1 < x_0 < 1$. Equation (13) is the standard form of the finite Hilbert transform. This transform occurs widely in problems in physics, and, consequently, a variety of numerical techniques have been proposed to evaluate this singular integral; see, for example, Bertie and Zhang [7]. Here we propose a specialized Gaussian quadrature scheme, which is straightforward to implement and provides accurate results.

To deal with Eq. (13), we will assume that $f(x)$ is Hölder continuous on the interval $[-1,1]$ with positive exponent m; that is,

$$|f(x - \varepsilon) - f(x + \varepsilon)| \le C|\varepsilon|^m, \tag{14}$$

where C is a positive constant. This constraint will be satisfied by all the continuous optical properties encountered in practical applications. Equation (13) can be recast as

$$\begin{aligned} K(x_0) &= \frac{1}{\pi}\lim_{\varepsilon\to 0}\left\{\int_{-1}^{x_0-\varepsilon} \frac{f(x)\mathrm{d}x}{x_0 - x} + \int_{x_0+\varepsilon}^{1} \frac{f(x)\mathrm{d}x}{x_0 - x}\right\} \\ &= \frac{1}{\pi}\lim_{\varepsilon\to 0}\left\{\int_{\varepsilon}^{1+x_0} \frac{f(x_0 - s)\mathrm{d}s}{s} - \int_{\varepsilon}^{1-x_0} \frac{f(x_0 + s)\mathrm{d}s}{s}\right\}, \end{aligned} \tag{15}$$

where the change of variables $s = x_0 - x$ and $s = x - x_0$ were employed in the first and second integrals, respectively. The function $K(x_0)$ can be rewritten as

$$\begin{aligned} K(x_0) &= \frac{1}{\pi}\lim_{\varepsilon\to 0}\int_{\varepsilon}^{1} \frac{\{f(x_0 - s) - f(x_0 + s)\}\mathrm{d}s}{s} \\ &\quad + \frac{1}{\pi}\left\{\int_{1}^{1+x_0} \frac{f(x_0 - s)\mathrm{d}s}{s} + \int_{1-x_0}^{1} \frac{f(x_0 + s)\mathrm{d}s}{s}\right\}. \end{aligned} \tag{16}$$

Employing an integration by parts allows the first integral in the preceding result to be expressed as

$$\begin{aligned} &\lim_{\varepsilon\to 0}\int_{\varepsilon}^{1} \frac{\{f(x_0 - s) - f(x_0 + s)\}\mathrm{d}s}{s} \\ &= \lim_{\varepsilon\to 0}\int_{\varepsilon}^{1} \{f(x_0 - s) - f(x_0 + s)\}\frac{\mathrm{d}\log_e s}{\mathrm{d}s}\mathrm{d}s \\ &= \lim_{\varepsilon\to 0}\left\{-[f(x_0 - \varepsilon) - f(x_0 + \varepsilon)]\log_e \varepsilon \right. \\ &\qquad \left. - \int_{\varepsilon}^{1} \log_e s\{f'(x_0 - s) - f'(x_0 + s)\}\mathrm{d}s\right\} \\ &= \int_{0}^{1} \log_e s^{-1}\{f'(x_0 - s) - f'(x_0 + s)\}\mathrm{d}s, \end{aligned} \tag{17}$$

where the prime denotes differentiation with respect to the variable s and the condition given in expression (14) has been employed to simplify the term $\lim_{\varepsilon\to 0}\log_e \varepsilon[f(x_0 - \varepsilon) - f(x_0 + \varepsilon)]$.

The other pair of integrals in Eq. (16) can be written in a form suitable for a Gauss–Legendre quadrature using the substitutions $s=1+\frac{1}{2}x_0(1+x)$ in the first of the pair and $s=1-\frac{1}{2}x_0(1+x)$ in the second integral, so that Eq. (13) can be expressed as

$$K(x_0)=\frac{1}{\pi}\int_0^1 \log_e x^{-1}\{f'(x_0-x)-f'(x_0+x)\}\mathrm{d}x + \frac{x_0}{\pi}\int_{-1}^1 \left\{\frac{f\left(\frac{x_0}{2}[1-x]-1\right)}{x_0(x+1)+2}-\frac{f\left(\frac{x_0}{2}[1-x]+1\right)}{x_0(x+1)-2}\right\}\mathrm{d}x. \tag{18}$$

Let

$$g_1(x_0,x)=\frac{1}{\pi}\{f'(x_0-x)-f'(x_0+x)\}, \tag{19}$$

$$g_2(x_0,x)=\frac{x_0}{\pi}\left\{\frac{f\left(\frac{x_0}{2}[1-x]-1\right)}{x_0(x+1)+2}-\frac{f\left(\frac{x_0}{2}[1-x]+1\right)}{x_0(x+1)-2}\right\}; \tag{20}$$

then

$$K(x_0)\approx\sum_{i=1}^{\bar{N}} g_1(x_0,\bar{x}_i)\bar{w}_i+\sum_{i=1}^{N} g_2(x_0,x_i)w_i, \tag{21}$$

where $\bar{x}_i$ and $\bar{w}_i$ denote the points and weights for a specialized Gaussian quadrature based on the weight function $\log_e x^{-1}$. The singular structure of the integrand in Eq. (13) is now submerged in the values $\bar{x}_i$ and $\bar{w}_i$. The number of evaluation points $\bar{N}$ for the specialized quadrature and the number N for the Gauss–Legendre quadrature need not be the same. In applications, N can be selected much larger than $\bar{N}$, simply because the availability of the $\{\bar{x}_i,\bar{w}_i\}$ values is rather limited.

The principal difficulty in implementing expression (21) is the determination of the weights $\bar{w}_i$ and abscissas $\bar{x}_i$ to high accuracy using the weight function $\log_e x^{-1}$. Values of $\{\bar{x}_i,\bar{w}_i\}$ for this particular choice of weight function can be found in the literature, but either the precision is somewhat limited or the size of $\bar{N}$ is rather modest [6,8,9]. In the present work the $\{\bar{x}_i,\bar{w}_i\}$ were determined from a standard recursive scheme [10]. Because this recursive scheme is well known to be numerically extremely unstable, it was necessary to resort to high-precision arithmetic. The calculations of the $\{\bar{x}_i,\bar{w}_i\}$ were carried out using the MATHEMATICA software. A modified recursive approach is available, with improved stability [10,11].

3. APPLICATIONS

Three examples were selected to test expression (21). Each of these examples was chosen because the resulting singular integral can be evaluated analytically, and hence a direct check on the numerical scheme is obtained. The choices also display a range of different functional behaviors. In practical applications, optical data could be fitted to rather general functional forms, for example, a ratio of power series (a Padé approximant), for which the resulting truncated Kramers–Kronig singular integral cannot be evaluated conveniently in analytic form.

Table 1 shows the results obtained from expression (21) for the selected test cases. The special functions [12] appearing in the table are the cosine integral, $\mathrm{Ci}(x)$,

$$\mathrm{Ci}(x)=-\int_x^\infty \frac{\cos y\mathrm{d}y}{y}; \tag{22}$$

the sine integral, $\mathrm{Si}(x)$,

$$\mathrm{Si}(x)=\int_0^x \frac{\sin y\mathrm{d}y}{y}; \tag{23}$$

the exponential integral, defined by

$$E_n(z)=\int_1^\infty \frac{e^{-zy}\mathrm{d}y}{y^n} \quad \text{for } n=0,1,2,\cdots, \quad \text{with } \mathrm{Re}\, z>0; \tag{24}$$

and the hyperbolic sine integral function,

$$\mathrm{Shi}(z)=\int_0^z \frac{\sinh t\mathrm{d}t}{t}. \tag{25}$$

The Gauss–Legendre quadrature was carried out using $N=384$, and the specialized Gaussian quadrature with the log weight was performed using $\bar{N}=60$. The number of points employed for the Gauss–Legendre quadrature was more than sufficient to achieve a high level of accuracy for the second integral in Eq. (18), for the test cases examined. This is expected to be the general case for optical properties, for which the kernel function of the second integral in Eq. (18) can be represented by a functional form that has an accurate polynomial approximation on the interval $(-1,1)$. There is the possibility of numerical prob-

Table 1. Comparison of Numerical Quadrature Values for the Finite Hilbert Transform versus Exact Evaluation[a]

$f(x)$	$\frac{1}{\pi}P\int_{-1}^{1}\frac{f(s)\mathrm{d}s}{x-s}$ (Exact Result)	Numerical Quadrature Result	From the Exact Result
x	$\frac{x}{\pi}\log\lvert\frac{1+x}{1-x}\rvert-\frac{2}{\pi}$	−0.4617701961	−0.4617701961
e^x	$\frac{e^x}{\pi}\{E_1(1-x)-E_1(1+x)-2\,\mathrm{Shi}(1-x)\}$	−0.2908672551	−0.2908672551
$\sin x$	$\frac{\sin x}{\pi}\{\mathrm{Ci}(1+x)-\mathrm{Ci}(1-x)\}-\frac{\cos x}{\pi}\{\mathrm{Si}(1+x)+\mathrm{Si}(1-x)\}$	−0.4088775094	−0.4088775094

[a]The evaluation point $x=\frac{1}{2}$ has been employed.

lems when the evaluation point x lies almost on the end points ± 1, though this will depend on the behavior of the kernel function as $x \to \pm 1$.

For the results presented in Table 1, the accuracy obtained was actually better than the number of digits reported. For typical optical data analysis, fewer significant figures will generally be required, compared with the number displayed in Table 1. Error estimates can be incorporated to improve the results; see Stroud and Secrest [6] for details. For the log-weighted quadrature, the required error coefficient has the value $3.74055842593670104809237 22 \times 10^{-73}$ for $(2\bar{N})! e_{2\bar{N}}$ using $\bar{N}=60$. For the test cases considered, error correction was unnecessary.

As a further example, we consider a popular oscillator model for the analysis of optical data [13]. Suppose the permittivity as a function of circular frequency is represented as

$$\varepsilon(\omega) - \varepsilon_\infty = \frac{\varepsilon_\infty(\omega_L^2 - \omega_T^2)}{\omega_T^2 - \omega^2 - i\Gamma\omega}; \tag{26}$$

then the real part $\varepsilon_r(\omega)$ and the imaginary part $\varepsilon_i(\omega)$ are given by

$$\varepsilon_r(\omega) - \varepsilon_\infty = \frac{\varepsilon_\infty(\omega_L^2 - \omega_T^2)(\omega_T^2 - \omega^2)}{(\omega_T^2 - \omega^2)^2 + \Gamma^2\omega^2}, \tag{27}$$

$$\varepsilon_i(\omega) = \frac{\varepsilon_\infty(\omega_L^2 - \omega_T^2)\Gamma\omega}{(\omega_T^2 - \omega^2)^2 + \Gamma^2\omega^2}. \tag{28}$$

In this model, ω_T, ω_L, ε_∞, and Γ are treated as flexible parameters to describe the particular optical constant under consideration. We have employed the values for GaAs, which are [13] $\omega_T = 268.7\ \mathrm{cm}^{-1}$, $\omega_L = 292.1\ \mathrm{cm}^{-1}$, $\varepsilon_\infty = 11.0\ \mathrm{cm}^{-1}$, and $\Gamma = 2.4\ \mathrm{cm}^{-1}$, and these describe the reststrahlen region of the spectrum. We have selected this example because it is possible to put the truncated Kramers–Kronig transforms in closed form, thus allowing a direct assessment of the quality of the numerical treatment of the corresponding truncated Kramers–Kronig transforms. Even slight modifications of Eq. (26) can quickly lead to intractable principal-value integrals.

The two Kramers–Kronig relations for the permittivity take the form

$$\varepsilon_i(\omega) = \frac{2\omega}{\pi} P \int_0^\infty \frac{[\varepsilon_r(\omega') - \varepsilon_\infty]\mathrm{d}\omega'}{\omega^2 - \omega'^2}, \tag{29}$$

$$\varepsilon_r(\omega) - \varepsilon_\infty = -\frac{2}{\pi} P \int_0^\infty \frac{\omega'\varepsilon_i(\omega')\mathrm{d}\omega'}{\omega^2 - \omega'^2}. \tag{30}$$

To evaluate the truncated Kramers–Kronig transform,

$$\varepsilon_r(\omega) - \varepsilon_\infty = -\frac{2}{\pi} P \int_{\omega_1}^{\omega_2} \frac{\omega'\varepsilon_i(\omega')\mathrm{d}\omega'}{\omega^2 - \omega'^2}, \tag{31}$$

we introduce the substitutions

$$a_2 = \frac{\omega_2}{\omega}, \quad a_1 = \frac{\omega_1}{\omega}, \quad a = \frac{\omega_T}{\omega}, \tag{32}$$

$$A = \omega_L^2 - \omega_T^2, \quad b = \frac{\Gamma}{2\omega}, \quad c = \sqrt{a^2 - b^2}, \tag{33}$$

so that, after some tedious algebra,

$$\begin{aligned}\varepsilon_r(\omega) - \varepsilon_\infty = \frac{A\varepsilon_\infty}{2\omega^2 c\pi}\Bigg\{ & b\Bigg(\frac{1}{(c+1)^2 + b^2} - \frac{1}{(c-1)^2 + b^2}\Bigg)\log_e\left[\frac{(1+a_2)(1-a_1)}{(a_2-1)(a_1+1)}\right] \\ & + \left\{\frac{(c-1)}{(c-1)^2 + b^2} + \frac{(c+1)}{(c+1)^2 + b^2}\right\} \\ & \times\left\{\tan^{-1}\left[\frac{a_2 - c}{b}\right] + \tan^{-1}\left[\frac{a_2 + c}{b}\right] - \tan^{-1}\left[\frac{a_1 - c}{b}\right] - \tan^{-1}\left[\frac{a_1 + c}{b}\right]\right\} \\ & + \frac{b}{2}\left\{\frac{1}{(c-1)^2 + b^2} + \frac{1}{(c+1)^2 + b^2}\right\} \\ & \times\left\{\log_e[(b^2 + (a_2 + c)^2)/(b^2 + (a_1 + c)^2)] - \log_e[(b^2 + (a_2 - c)^2)/(b^2 + (a_1 - c)^2)]\right\}\Bigg\}.\end{aligned} \tag{34}$$

In the limits $\omega_1 \to 0$ (that is, $a_1 \to 0$) and $\omega_2 \to \infty$ (that is, $a_2 \to \infty$), the first logarithm term and also the pair of logarithm terms in the preceding formula vanish, the sum of the first two arctangents gives a contribution of π, and the sum of the third and fourth arctangents cancels, so that Eq. (34) simplifies to

$$\varepsilon_r(\omega) - \varepsilon_\infty = \frac{A\varepsilon_\infty}{2\omega^2 c}\left\{\frac{(c-1)}{(c-1)^2 + b^2} + \frac{(c+1)}{(c+1)^2 + b^2}\right\}. \tag{35}$$

A short rearrangement of Eq. (35) leads to

$$\varepsilon_r(\omega) - \varepsilon_\infty = \frac{A\varepsilon_\infty}{\omega^2}\frac{(a^2 - 1)}{(a^2 - 1)^2 + 4b^2}, \tag{36}$$

which corresponds to Eq. (27).

The truncated Kramers–Kronig transform for $\varepsilon_i(\omega)$ is

$$\varepsilon_i(\omega) = \frac{2\omega}{\pi} P \int_{\omega_1}^{\omega_2} \frac{[\varepsilon_r(\omega') - \varepsilon_\infty]\mathrm{d}\omega'}{\omega^2 - \omega'^2}, \tag{37}$$

and, for the oscillator model, it can be worked out in closed form, with the result that

$$\begin{aligned}\varepsilon_i(\omega) = \frac{A\varepsilon_\infty}{2\omega^2 c\pi}\Bigg\{ & \Bigg(\frac{c+1}{(c+1)^2 + b^2} + \frac{c-1}{(c-1)^2 + b^2}\Bigg)\log_e\left[\frac{(1+a_2)(1-a_1)}{(a_2-1)(a_1+1)}\right] \\ & + b\left\{\frac{1}{(c-1)^2 + b^2} - \frac{1}{(c+1)^2 + b^2}\right\}\left\{\tan^{-1}\left[\frac{a_2 + c}{b}\right]\right.\end{aligned}$$

$$- \tan^{-1}\left[\frac{a_1 + c}{b}\right] + \tan^{-1}\left[\frac{a_2 - c}{b}\right] - \tan^{-1}\left[\frac{a_1 - c}{b}\right]$$
$$+ \frac{1}{2}\left\{\frac{c+1}{(c+1)^2 + b^2} - \frac{c-1}{(c-1)^2 + b^2}\right\}$$
$$\times\{\log_e[(b^2 + (a_2 + c)^2)/(b^2 + (a_1 + c)^2)]$$
$$- \log_e[(b^2 + (a_2 - c)^2)/(b^2 + (a_1 - c)^2)]\}. \quad (38)$$

Taking the limits $\omega_1 \to 0$ and $\omega_2 \to \infty$ in Eq. (38) leads to Eq. (28).

The approach presented in Section 2 is applied to evaluate the truncated Kramers–Kronig transforms given in Eqs. (31) and (37), using the oscillator model applied to the GaAs data. The results for the determination of $\varepsilon_r(\omega) - \varepsilon_\infty$ are displayed in Fig. 1, calculated assuming truncation intervals of $\omega_1 = 100$ cm^{-1} and $\omega_2 = 320$ cm^{-1}. This is a fairly narrow range but does incorporate all the essential structure in the real and imaginary components of the permittivity, using the given data for GaAs in the reststrahlen region of the spectrum.

For a given value of ω, a split of the integration interval was tested, to ensure the quadrature result was accurate to within a preselected tolerance. Given the precision of the data for GaAs, an accuracy tolerance of about 0.1% would be sufficient; for the calculations we report in the figures, an accuracy tolerance of 0.001% was employed. Further splitting of the integration interval was automated, so that the accuracy of the quadrature was below the set tolerance. For most values of the circular frequency, this was accomplished without splitting the interval for the nonsingular parts of the integral and with minimum or no splitting for the singular part of the integral.

In Fig. 1, the quadrature determination of $\varepsilon_r(\omega) - \varepsilon_\infty$ from the truncated Kramers–Kronig transform is compared with the result from the exact solution, Eq. (34). The two results are observed to be superimposed, thus establishing the effectiveness of the quadrature approach presented. As a parenthetical comment, we note that the exact result for $\varepsilon_r(\omega) - \varepsilon_\infty$ from Eq. (27) differs slightly from the truncated Kramers–Kronig result. This behavior is clearly evident in Fig. 1.

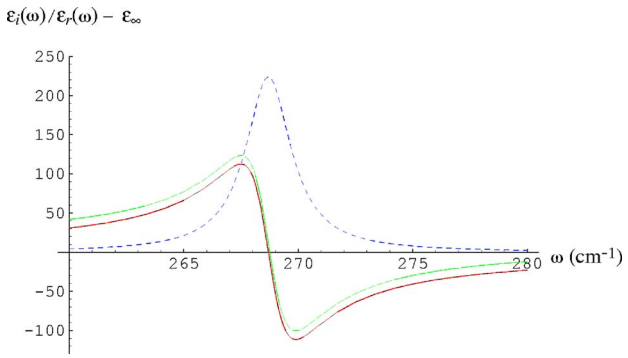

Fig. 1. (Color online) Numerical quadrature result for $\varepsilon_r(\omega) - \varepsilon_\infty$. The values of $\varepsilon_r(\omega) - \varepsilon_\infty$ from the exact result, Eq. (27), are represented by the long-dashed curve. The input $\varepsilon_i(\omega)$ for the numerical quadrature is represented by the short-dashed curve. The solid curve is the numerical quadrature result superimposed on the exact result for the truncated Kramers–Kronig transform from Eq. (34).

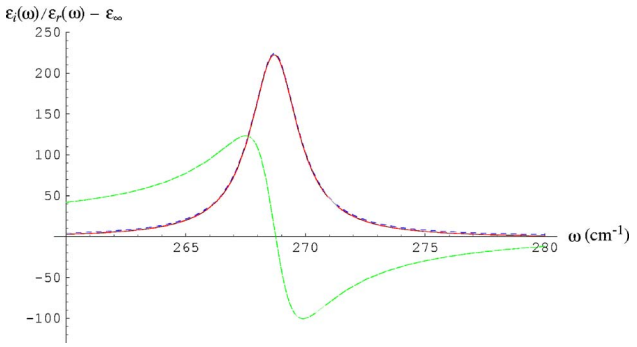

Fig. 2. (Color online) Numerical quadrature result for $\varepsilon_i(\omega)$. The values of $\varepsilon_i(\omega)$ from the exact result, Eq. (28), are represented by the short-dashed curve. The input $\varepsilon_r(\omega) - \varepsilon_\infty$ for the numerical quadrature is represented by the long-dashed curve. The solid curve is the numerical quadrature result superimposed on the exact result for the truncated Kramers–Kronig transform from Eq. (38).

The results for the quadrature determination of $\varepsilon_i(\omega)$ from the truncated Kramers–Kronig formula, Eq. (37), are displayed in Fig. 2. The quadrature result and the exact result from Eq. (38) are superimposed upon each other. The exact result for $\varepsilon_i(\omega)$ from Eq. (28) is also included in the figure as a useful reference. This latter result coincides closely with the other two results—with some small departures evident in the tails on both sides of the $\varepsilon_i(\omega)$ maximum. The better agreement between the exact and the truncated Kramers–Kronig transform results for the case of $\varepsilon_i(\omega)$, as compared with the behavior for $\varepsilon_r(\omega) - \varepsilon_\infty$, is due to the faster falloff of $\varepsilon_i(\omega)$ as a function of increasing circular frequency, thus leading to smaller errors when the truncation of the Kramers–Kronig transform is carried out.

A nonoptimized FORTRAN code used for the evaluation of the truncated Kramers–Kronig transform for a typical set of values of ω, ω_1, and ω_2 outperforms the CAUCHYPRINCIPALVALUE numerical integration function in MATHEMATICA, by a factor of approximately 100 in terms of CPU usage. This reflects in part the known computational overhead of compiled MATHEMATICA functions. Since the calculation of individual integrals for a given set of ω, ω_1, and ω_2 values is substantially less than a second, CPU considerations are not much of an issue. The more important consideration is accuracy. The CAUCHYPRINCIPALVALUE function gives reasonably good accuracy, provided that the function under investigation does not exhibit relatively rapid changes in the integration interval. For the oscillator model, numerical experiments using the CAUCHYPRINCIPALVALUE function indicate a loss of accuracy as the dissipative profile of the permittivity was modified by decreasing the value of the damping constant Γ. The algorithm of Section 2 was able to handle this change without difficulty, as judged by comparison with the results produced from the exact truncated Kramers–Kronig transform.

4. DISCUSSION

For functions that lead to kernels in Eq. (18) that can be well approximated by a polynomial of limited degree, the quadrature approach outlined will be effective. Using 60

Table 2. Abscissas and Weights for a Gaussian Quadrature with a Weight Function of $\log_e x^{-1}$ for $\bar{N}=60$

Abscissas ($\bar{x}_i$)	Weights ($\bar{w}_i$)
0.3242993314 4248107289 12086753 E-03	0.7155181881 1300426417 62569777 E-02
0.1860416905 5784504158 15950880 E-02	0.1373694600 1689768187 39119679 E-01
0.4696573639 0991652078 39421141 E-02	0.1869537888 1776323261 40629494 E-01
0.8833904836 9572925024 05254807 E-02	0.2263474845 1526893488 03176064 E-01
0.1426594295 0014852993 59075483 E-01	0.2582207148 4993127288 09788143 E-01
0.2098127619 9176948993 75918976 E-01	0.2840945573 6376243830 23740854 E-01
0.2896429015 1974968507 77796613 E-01	0.3049634644 8417452363 64635613 E-01
0.3819550862 7577167845 76524517 E-01	0.3215378277 2867450134 83128685 E-01
0.4865179933 4554167127 17892587 E-01	0.3343582004 8381905227 23927553 E-01
0.6030652447 3874537777 99581031 E-01	0.3438560534 1658051990 39257271 E-01
0.7312966757 2377715272 19560949 E-01	0.3503889570 1292293530 72188840 E-01
0.8708795071 6818465500 47868478 E-01	0.3542622661 8137415111 60834543 E-01
0.1021449492 7718703334 37534345	0.3557431317 9722807461 68939944 E-01
0.1182612079 0207493527 67365360	0.3550698901 9998310718 19109188 E-01
0.1353943598 7942803410 62150527	0.3524585360 1232078426 25832897 E-01
0.1534992510 2791649982 44103932	0.3481072831 2964683853 77116284 E-01
0.1725280687 4247676881 07516152	0.3421998324 7375104565 33520258 E-01
0.1924304764 8440543587 94060473	0.3349077416 9485313548 99206955 E-01
0.2131537537 9162642166 49791475	0.3263921574 4805421225 31608779 E-01
0.2346429417 4030179976 88820397	0.3168050869 5948533893 63340905 E-01
0.2568409936 8793538512 01640973	0.3062903316 6486108988 64536888 E-01
0.2796889310 5491968614 55351222	0.2949841701 0523366161 83963033 E-01
0.3031260038 4673172558 90597421	0.2830158532 0746897358 54189801 E-01
0.3270898555 7690101950 71618612	0.2705079584 7117274794 61080971 E-01
0.3515166922 1778264157 37389705	0.2575766378 9968035821 51906590 E-01
0.3763414547 7968952572 17397767	0.2443317861 4624767855 67389969 E-01
0.4014979950 9749646457 95562510	0.2308771492 5795409049 59389643 E-01
0.4269192543 8636326868 53936516	0.2173103899 0143052525 78216135 E-01
0.4525374441 1401036027 93196121	0.2037231215 8329769188 99028894 E-01
0.4782842287 2551210517 52776207	0.1902009218 1711193980 25609730 E-01
0.5040909097 4749546810 89911828	0.1768233322 1730712784 24231726 E-01
0.5298886107 9168916656 71621170	0.1636638519 6378294852 73754391 E-01
0.5556084629 7277580090 61005602	0.1507899298 6756158028 59216140 E-01
0.5811817902 5231879837 89849734	0.1382629592 9824698944 60722438 E-01
0.6065402942 1906302504 31149301	0.1261382794 4941953790 76135105 E-01
0.6316162378 1606124476 92522564	0.1144651857 7548128854 46957183 E-01
0.6563426275 2679276478 30505384	0.1032869519 0076314604 93804968 E-01
0.6806533935 3566088849 86063477	0.9264086485 4849783331 65202495 E-02
0.7044835673 8293455484 58207044	0.8255827510 8878508270 69568103 E-02
0.7277694566 4029349689 04441159	0.7306466256 2173184923 01686737 E-02
0.7504488161 4060444129 26572297	0.6417971934 6374123518 26380248 E-02
0.7724610153 0435804028 93767166	0.5591745006 7047158592 38924556 E-02
0.7937472011 1529142145 35345932	0.4828628988 4274780594 39472622 E-02
0.8142504563 0906633852 22587269	0.4128924063 9033490732 27806408 E-02
0.8339159523 5142074989 45672602	0.3492402505 7411225839 44405848 E-02
0.8526910967 9590805452 69922043	0.2918325890 6919565532 41258132 E-02
0.8705256746 2611647352 99979058	0.2405464083 5959599528 52300011 E-02
0.8873719832 0303087598 55773764	0.1952115949 7066545695 73897805 E-02
0.9031849604 5482295781 03094573	0.1556131743 5442202694 35263614 E-02
0.9179223059 6359360185 33336050	0.1214937111 5354054258 44980658 E-02
0.9315445946 2097135151 50164879	0.9255586357 3497100062 22011536 E-03
0.9440153825 4095212996 78639651	0.6846508368 2151985039 66829933 E-03
0.9553013049 3140747807 62997290	0.4885245462 6620370345 95480646 E-03
0.9653721656 2844728181 58690176	0.3331765500 4587598419 89636978 E-03
0.9742010179 6975726056 16350959	0.2143203994 8545842187 36594045 E-03
0.9817642365 5412274904 05066658	0.1274182787 6086249031 91376689 E-03
0.9880415789 2436265047 76861980	0.6771381333 3216217294 81754795 E-04
0.9930162339 2887477895 28321127	0.3026569953 0513963209 42851280 E-04
0.9966748400 1858749516 02439285	0.9982035828 0485052441 39485304 E-05
0.9990073230 8937402711 32293595	0.1655280633 5491778653 48936290 E-05

quadrature points for the weight function $\log_e x^{-1}$ gives good accuracy in these cases. The weights and abscissas for $\bar{N}=60$ are reproduced in Table 2. For functions that cannot be so represented, the accuracy of the approach is likely to be more modest but probably sufficiently accurate for analysis of optical data. Typical optical properties are expected to be well approximated on any finite spectral interval by functions for which the series representation of the kernels of Eq. (18) is accurately represented by a polynomial approximation.

A useful evaluation strategy is to first check that the kernel functions that arise in Eq. (18) can be expanded in a series form for $x \in (0,1)$ for the first integral and $x \in (-1,1)$ for the second integral. Then check that these series are well approximated by polynomials of modest degree, that is, a polynomial of size $\approx 2\bar{N}$ for the kernel of the first integral in Eq. (18) and $\approx 2N$ for the kernel of the second integral in the same equation. Abscissas and weights for the Gauss–Legendre quadrature are available to rather high order; however, for the log quadrature, determination of the abscissas and weights for values of $\bar{N}$ in excess of 100 becomes problematic, particularly if these are to be determined to high accuracy. The author has determined the $\{\bar{x}_i, \bar{w}_i\}$ values for $\bar{N}$ from 10 to 100 in steps of 10. The values for $\{\bar{x}_i, \bar{w}_i\}$ for $\bar{N}$ greater than 60 can be obtained by contacting the author. The convergence of the quadrature approach can be monitored by successively increasing the size of $\bar{N}$ and N. An alternative approach is to split the integration interval of the initial truncated Kramers–Kronig transform into two or more segments. This can be carried out in an automated fashion and terminated when a required cutoff tolerance is reached.

A related approach can be carried out for the Hilbert transform on the interval $(-\infty, \infty)$. For the case of functions that have reasonably good decay characteristics, the specialized Gaussian quadrature approach produces accurate results [14].

Partial support from the Petroleum Research Fund of the American Chemical Society is greatly appreciated.

REFERENCES

1. K.-E. Peiponen, E. M. Vartiainen, and T. Asakura, *Dispersion, Complex Analysis and Optical Spectroscopy* (Springer, 1999).
2. D. E. Aspnes, "The accurate determination of optical properties by ellipsometry," in *Handbook of Optical Constants of Solids*, E. D. Palik, ed. (Academic, 1985), pp. 89–112.
3. V. Lucarini, J. J. Saarinen, K.-E. Peiponen, and E. M. Vartiainen, *Kramers–Kronig Relations in Optical Materials Research* (Springer-Verlag, 2005).
4. V. Lucarini and K.-E. Peiponen, "Verification of generalized Kramers–Kronig relations and sum rules on experimental data of third harmonic generation susceptibility on polymer," J. Chem. Phys. **119**, 620–627 (2003).
5. V. Lucarini, J. J. Saarinen, and K.-E. Peiponen, "Multiply subtractive Kramers–Krönig relations for arbitrary-order harmonic generation susceptibilities," Opt. Commun. **218**, 409–414 (2003).
6. A. H. Stroud and D. Secrest, *Gaussian Quadrature Formulas* (Prentice Hall, 1966).
7. J. E. Bertie and S. L. Zhang, "Infrared intensities of liquids. IX. The Kramers–Kronig transform, and its approximation by the finite Hilbert transform via fast Fourier transforms," Can. J. Chem. **70**, 520–531 (1992).
8. V. I. Krylov and A. A. Pal'cev, "Numerical integration of functions having logarithmic and power singularities," Vestsi Akad. Navuk BSSR, Ser. Fiz.-Tekh. Navuk 14–23 (1963).
9. B. Danloy, "Numerical construction of Gaussian quadrature formulas for $\int_0^1(-\mathrm{Log}\,x)\cdot x^{\alpha}\cdot f(x)\cdot \mathrm{d}x$ and $\int_0^1 E_m(x)\cdot f(x)\cdot \mathrm{d}x$," Math. Comput. **27**, 861–869 (1973).
10. W. H. Press, S. A. Teukolsky, W. T. Vetterling, and B. P. Flannery, *Numerical Recipes in FORTRAN 77*, 2nd ed. (Cambridge U. Press, 1992).
11. R. A. Sack and A. F. Donovan, "An algorithm for Gaussian quadrature given modified moments," Numer. Math. **18**, 465–478 (1972).
12. M. Abramowitz and I. A. Stegun, *Handbook of Mathematical Functions* (Dover, 1965).
13. E. D. Palik, "Gallium arsenide (GaAs)," in *Handbook of Optical Constants of Solids*, E. D. Palik, ed. (Academic, 1985), p. 429.
14. F. W. King, "Efficient numerical approach to the evaluation of Kramers–Kronig transforms," J. Opt. Soc. Am. B **19**, 2427–2436 (2002).